



Base-Free Generation of Organic Electron Donors from Air-Stable Precursors

Guillaume Tintori, Pierre Nabokoff, Ruqaya Buhaibeh, David Bergé-Lefranc, Sébastien Redon, Julie Broggi, Patrice Vanelle

► To cite this version:

Guillaume Tintori, Pierre Nabokoff, Ruqaya Buhaibeh, David Bergé-Lefranc, Sébastien Redon, et al.. Base-Free Generation of Organic Electron Donors from Air-Stable Precursors. *Angewandte Chemie International Edition*, 2018, *Angewandte Chemie International Edition*, 57 (12), pp.3148-3153. <10.1002/anie.201713079>. <hal-02079702>

HAL Id: hal-02079702

<https://amu.hal.science/hal-02079702v1>

Submitted on 18 Feb 2021

HAL is a multi-disciplinary open access archive for the deposit and dissemination of scientific research documents, whether they are published or not. The documents may come from teaching and research institutions in France or abroad, or from public or private research centers.

L'archive ouverte pluridisciplinaire **HAL**, est destinée au dépôt et à la diffusion de documents scientifiques de niveau recherche, publiés ou non, émanant des établissements d'enseignement et de recherche français ou étrangers, des laboratoires publics ou privés.



HAL Authorization

Base-free generation of organic electron donors from air-stable precursors

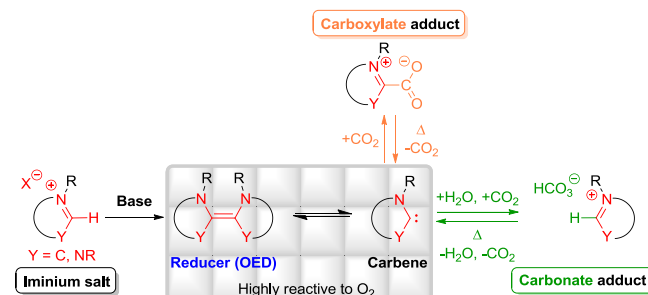
Guillaume Tintori,^[a] Pierre Nabokoff,^[a] Ruqaya Buhaibeh,^[a] David Bergé-Lefranc,^[b] Sébastien Redon,^[a] Julie Broggi^{*[a]} and Patrice Vanelle^{*[a]}

Abstract: Organic electron donors (OEDs) are powerful reducing agents recognized for their potential in the reduction of challenging substrates and in original applications. Nonetheless, their stability issues in atmospheric oxygen or over time complicate their manipulation and storage. To overcome these constraints and enhance OED's practicality, new air- and moisture-stable aminopyridinium carboxylate and carbonate precursors were synthesized and thermally activated to *in-situ* generate the potent electron donor. Carboxylate adducts proved to be excellent OED-latent systems allowing easy and efficient reduction of challenging substrates. Their reducing properties are correlated to their structural characteristics by thermogravimetric and spectrometric analysis.

Organic electron donors (OEDs) with exceptionally negative redox potentials showed their potency and chemoselectivity in the reduction of challenging substrates.¹ They promote the formation of radical or anionic intermediates by single- or double-electron transfers.² These strong reducing agents are now attracting more and more the interest for original applications in diverse domains (coupling partners, polymerization initiators, redox switches, greenhouse gas reduction).³ Their structures usually consist of two aza-cycles, such as imidazole or pyridine rings, connected at their center by an electron-rich double bond (Scheme 1). Typically, the enamine is prepared by addition of a strong base (NaH, KHMDS) on the cyclic iminium precursor salt. Some enamines (such as **OED-2**, Scheme 2) are stable under inert atmosphere and can be stored and manipulated in a glove box.⁴ In other cases, the dimeric form is elusive (**OED-1** has a half-life time of few minutes) and is rapidly converted into the corresponding carbene (**Cb-1**).⁵ Thanks to the great resonance stabilization of their oxidized forms, pyridine and imidazole derivatives are powerful reducing agents with $E_{1/2}$ (**OED-2**) = -1.27 V and $E_{1/2}$ (**OED-1**) ≈ -1.20 V vs. SCE. To deal with stability issues, one solution is to *in-situ* generate the electron donor from the iminium salt in the presence of the substrate to be reduced. However, the concomitant use of excess amount of strong base is problematic as it presents limited tolerance to various functionalities and often gives complex mixtures.

To overcome these constraints and enhance OED's

practicality, new strategies based on the activation of air- and moisture-stable masked OED-systems are crucial for the easy and efficient generation of organic reducers (Scheme 1). Our choice went to the use of carboxylate and carbonate adducts, well-known carbene precursors.⁶ The advantage of these adducts is that any types of structures are virtually accessible by reaction of free *N*-heterocyclic carbenes (NHC) with CO₂ atmosphere or by anion metathesis of azolium halides. Their thermolysis *in-situ* regenerate the free NHCs by decarboxylation, and CO₂ is the only byproduct. This study proves that organic electron donors can also be formed during the process of thermal activation of carboxylate and carbonate adducts.



Scheme 1. *In-situ* generation of OEDs.

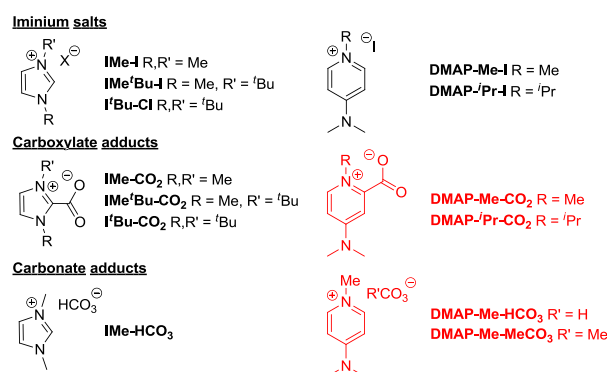


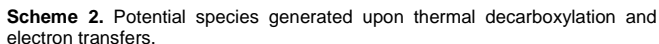
Figure 1. OED-precursors used in this study (new structures in red).

Synthesis and characterization of OED-precursors

All new carboxylate and carbonate precursors of pyridinylidene-type reducers (**DMAP-series**) were synthesized in good yields using similar strategies than the ones reported for imidazolium-based carboxy adducts (**I-series** in Figure 1).^{7,8} Functionalization of the dimethylamino-pyridine core (DMAP) was obtained by a two-step procedure involving the deprotonation of the pyridinium

[a] G. Tintori, P. Nabokoff, R. Buhaibeh, Dr. S. Redon, Dr. J. Broggi, Prof. P. Vanelle
Aix-Marseille Univ, CNRS, Institut de Chimie Radicalaire ICR
Faculté de Pharmacie,
Marseille, France.
E-mail: julie.broggi@univ-amu.fr; patrice.vanelle@univ-amu.fr.
^a Both authors contributed equally to this work.

[b] Dr. D. Bergé-Lefranc
Aix-Marseille Univ, CNRS, IRD, Laboratoire IMBE UMR 7263
Faculté de Pharmacie,
Marseille, France.



4-substituted 1,2,3,4-tetrahydropyridine $\xrightarrow[\text{CH}_3\text{CN}, 70 \text{ or } 100^\circ\text{C}]{\text{RI}}$ 4-substituted 1,2,3,4-tetrahydropyridinium salt

4-substituted 1,2,3,4-tetrahydropyridine $\xrightarrow[\text{MeOH}, 120^\circ\text{C}, 60\text{h}]{\text{MeOH}}$ 4-substituted 1,2,3,4-tetrahydropyridinium salt

4-substituted 1,2,3,4-tetrahydropyridinium salt $\xrightarrow[\text{rt}, 12\text{h}]{\text{1) KHMDS, THF, rt, 1h; 2) CO}_2 \text{ (1 atm)}}$ 4-substituted 1,2,3,4-tetrahydropyridinium salt with carboxylate

4-substituted 1,2,3,4-tetrahydropyridinium salt with carboxylate $\xrightarrow[\text{rt}, 36\text{h}]{\text{H}_2\text{O, EtOH}}$ 4-substituted 1,2,3,4-tetrahydropyridinium salt with carboxylate

Yields:

- DMAP-Me-I, 99%
- DMAP-*Pr*-I, 99%
- DMAP-Me-CO₂, 70%
- DMAP-*Pr*-CO₂, 70%
- DMAP-Me-MeCO₃, 97%
- DMAP-Me-HCO₃, 88%

Structures of **DMAP-Me-CO₂**, **DMAP-ⁱPr-CO₂** and **DMAP-Me-HCO₃** were confirmed by single crystal X-ray crystallography and compared to the data reported for the imidazolium counterparts (Table 1 and 2).^{8,10} Louie demonstrated that imidazolium carboxylates had a great resonance stabilization when the CO₂ lay in the same plane as the imidazolium ring. On the other hand, an increase in *N*-substituent size clearly induced longer C-CO₂ bond and higher torsional angles, thus causing decreased stability of the NHC-CO₂ and lower decarboxylation temperatures. In our case, the C-CO₂ bond lengths of **DMAP-Me-CO₂** and **DMAP-ⁱPr-CO₂** (1.53 Å and 1.529 Å, respectively) were longer than in **IME-CO₂** (1.523 Å) but shorter than in **ⁱBu-CO₂** (1.551 Å). As well, the carboxylate torsional

Table 1. X-ray and structural features of NHC-CO₂.



| IRR' adduct | - CO₂ temp (°C) | DMAP-R adduct | - CO₂ temp (°C) |
|-------------------------------------|-----------------------------------|---------------------------|-----------------------------------|
| Ime-CO ₂ | 140 | DMAP-Me-CO ₂ | 181 |
| Ime-HCO ₃ | 40, 130 | DMAP-Me-HCO ₃ | 55, 117 |
| Ime ^t Bu-CO ₂ | 113 | DMAP-Me-MeCO ₃ | 34, 110 |

Thermogravimetric analysis (TGA) further confirmed these conclusions showing intermediate decarboxylation temperatures for pyridinium derivatives (**DMAP-Me-HCO₃**: 117°C, **DMAP-Me-MeCO₃**: 110°C, **DMAP-*i*Pr-CO₂**: 103°C, Table 2 and Figure S1-S2).¹¹ The first phenomena observed at 40, 55 and 34°C for **IMe-HCO₃**, **DMAP-Me-HCO₃** and **DMAP-Me-MeCO₃** corresponded to the prior loss of a molecule of H₂O or MeOH (10, 6 and 15% of mass loss, respectively). Surprisingly, **DMAP-Me-CO₂** presented a much higher decomposition temperature (181°C). Its crystalline structure displays an orthorhombic cell with a perfect alignment of the amino-pyridiniums compared to the monoclinic crystalline structures of **DMAP-*i*Pr-CO₂** and **DMAP-Me-HCO₃**.¹¹ The well-organized arrangement of **DMAP-Me-CO₂** improves atom interactions and confers a particular rigidity to the solid that might explain its higher thermal resistance by TGA. The crystallographic program PLATON© confirmed the presence of twice hydrogen bond interactions in **DMAP-Me-CO₂** compared to **DMAP-*i*Pr-CO₂** and **DMAP-Me-HCO₃**.¹¹ In solution, however, **DMAP-Me-CO₂** have a better reactivity at 120°C than **DMAP-*i*Pr-CO₂** (*vide infra* Table 4, entry 8 vs. 11).¹² Given the low steric bulk around the CO₂ unit, the breakability of the C-CO₂ bond in amino-pyridinium carboxylates seemed more related to the electronic influence of the amino-pyridine ring rather than the steric effect of the *N*-substituent. As a matter of fact, introduction of the bulkier isopropyl group (**DMAP-*i*Pr-CO₂**) had little impact on the structural features and the decarboxylation temperature. Unfortunately, preparation of a *tert*-butyl analog, for the observation of a possible combined electronic and steric effect, failed.

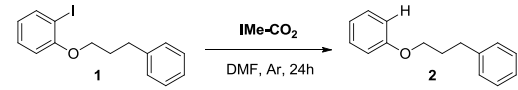
Comparative study for the reduction of 1

Different temperatures of decarboxylation were first compared using the readily accessible and well-documented 1,3-dimethylimidazolium-2-carboxylate (**IMe-CO₂**)⁷ as OED-precursor (Table 3). Below 150°C, reduction of the 1-iodo-2-(3-phenoxypropyl)benzene **1**, a benchmark substrate in OED-promoted reduction, was zero or close to it (Entries 1-2) even assisted by microwave irradiations (Entry 3).¹³ At 150°C, a good conversion (74%) into the reduced product **2** was observed (Entry 4). This temperature threshold is of the same order as the decarboxylation temperature measured by TGA for **IMe-CO₂** (Table 2). The drastic fall in conversion rate (19%) in a sealed system also confirmed the necessity for the loss of the CO₂ gas (Entry 5). For a complete reduction of **1**, several options were possible (for details see Table S1 in supporting information): i) the reaction time could be lengthened to 48h; ii) the quantity of precursor could be increased to 6 equivalents; iii) the flask could be purged with vacuum/N₂ cycles performed at 150°C at the beginning of the reaction. This vacuum effect, certainly leading to better removal of the CO₂, was not sufficient to decrease the reaction temperature or the precursor equivalents; iv) the solvent concentration could be increased to 0.08 M (Table 3, entry 6). This last option had a greater impact, allowing the reduction of **IMe-CO₂** loading to 3 equivalents (Entry 7). Note that the use of 3 equivalents of carboxylate adduct imply the *in-situ* generation of only 1.5 equivalents of OED with respect to the substrate. Even tough preparation of these reaction mixtures was

performed in a glove-box for a more accurate comparative study, a full conversion was also obtained when the reaction was set-up in air and degassed under N₂ before heating (Entry 9).

Different carboxylate and carbonate adducts were then compared expecting that the easy decarboxylation profile of *N*-hindered imidazolium carboxylates, such as ***i*Bu-CO₂**, would allow the reduction of **1** at lower temperatures (Table 4). Unfortunately, a linear decrease in conversion rates was observed as the bulk of the *N*-substituents increased (Entries 2-6). Knowing that the decarboxylation of these imidazolium adducts is not a problem at these working temperatures,⁸ the steric hindrance around the N₂C-carbon center seems to be a serious impediment to the generation of the corresponding OED dimeric form. As predicted by our structural analysis, aminopyridinium adducts, **DMAP-Me-CO₂** and **DMAP-*i*Pr-CO₂**, were better candidates: At 120°C, higher conversion rates were obtained (68 and 15%, respectively – Entries 8 and 11) than with **IMe-CO₂** (6% – Table 3, entry 2). Moreover, after 6h at 150°C, 90% conversion into **2** was reached with **DMAP-Me-CO₂** versus 36% for **IMe-CO₂** (Entries 1 and 9).

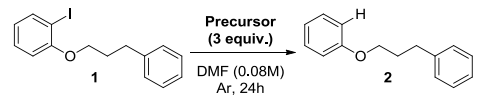
Table 3. Optimization of the reduction of **1**.^[a]



| Entry | IMe-CO₂ (equiv.) | Temp. (°C) | Concentration (mol.l ⁻¹) | Conv. (%) ^[b] |
|-------|------------------------------------|--------------------|--------------------------------------|--------------------------|
| 1 | 5 | 80 | 0.04 | 0 |
| 2 | 5 | 120 | 0.04 | 6 |
| 3 | 5 | 120 ^[c] | 0.04 | 6 |
| 4 | 5 | 150 | 0.04 | 74 |
| 5 | 5 | 150 ^[d] | 0.04 | 19 |
| 6 | 5 | 150 | 0.08 | >99 |
| 7 | 3 | 150 | 0.08 | >99 (87) |
| 8 | 2 | 150 | 0.08 | 78 |
| 9 | 3 | 150 ^[e] | 0.08 | 95 |

[a] **1** (1 equiv.), **IMe-CO₂** (2-5 equiv.), DMF (0.04 or 0.08 M), Ar, 24h. [b] ¹H NMR conversion (isolated yield). [c] Microwave heating, 16h. [d] Closed schlenk. [e] Set-up in air and degassed under N₂ before heating.

Table 4. Comparison of different carboxylate and carbonate precursors.^[a]



| Entry | Precursor | Temperature (°C) | Conv. (%) ^[b] |
|-------|--|------------------|--------------------------|
| 1 | IMe-CO₂ | 150 | 36 ^[c] |
| 2 | IMe-CO₂ | 150 | >99 |
| 3 | IMe^{<i>i</i>}Bu-CO₂ | 120 | 0 |
| 4 | IMe^{<i>i</i>}Bu-CO₂ | 150 | 36 |
| 5 | <i>i</i>Bu-CO₂ | 70 | 0 |
| 6 | <i>i</i>Bu-CO₂ | 150 | 22 |
| 7 | IMe-HCO₃ | 150 | 59 |
| 8 | DMAP-Me-CO₂ | 120 | 68 |
| 9 | DMAP-Me-CO₂ | 150 | 90 ^[c] |
| 10 | DMAP-Me-CO₂ | 150 | >99 (80) |
| 11 | DMAP-<i>i</i>Pr-CO₂ | 120 | 15 |
| 12 | DMAP-<i>i</i>Pr-CO₂ | 150 | >99 |

| | | | |
|----|---------------------------------|-----|----|
| 13 | DMAP-Me-HCO₃ | 150 | 76 |
| 14 | DMAP-Me-MeCO₃ | 120 | 42 |
| 15 | DMAP-Me-MeCO₃ | 150 | 88 |

[a] **1** (1 equiv.), precursor (3 equiv.), DMF (0.08 M), Ar, 24h. [b] ¹H NMR conversion (isolated yield). [c] Reaction time: 6h.

As expected from TGA, the impact of the bulkier *N*-isopropyl group on the decarboxylation and reactivity of **DMAP-ⁱPr-CO₂** (Entries 11-12) was not as evident as in imidazole series. Hydrogen carbonate adducts **IMe-HCO₃** and **DMAP-Me-HCO₃** could also be used as OED-precursors but they were less efficient than their carboxylate counterparts (Entries 7 and 13). **DMAP-Me-MeCO₃** gave a good percentage of product **2** (88% - Entry 15) but this carbonate salt was sensitive to water and rapidly decomposed into **DMAP-Me-HCO₃** upon exposure to air.

Evidence supporting the involvement of an organic donor

First, decarboxylation of the precursor is required as highlighted by the initiation of reactivity at high temperatures or inhibition of the reduction of **1** in closed systems (Table 3). This raises the question about the nature of the generated active species: carbene or enamine? Based on the preferential form adopted in the Wanzlick equilibrium upon deprotonation of the cyclic iminium salt,^{4,5} *in-situ* decarboxylation of **IMe-CO₂** should mainly lead to the formation of the carbene **Cb-1**, while **DMAP-Me-CO₂** should give **OED-2** (Scheme 2). In the literature, there is no report on reaction of free carbenes on iodoarenes,¹⁴ while their reduction with organic reducers such as **OED-1** and **OED-2** is reported.^{4b,5a} Indeed, almost no reaction occurred using **Cb-1** at room temperature (Table 5, Entry 2), while reduction of **1** was complete using the powerful organic reducer **OED-2** (Entry 1). Interestingly, at 150°C, partial reduction of **1** was observed in the presence of **Cb-1** (Entry 3). Two mechanisms could be considered starting from **IMe-CO₂** (Scheme 2): 1) At this high temperature, according to Van't Hoff law, the proportion of dimer **OED-1** will be even lower than at room temperature. However, the electron transfer from **OED-1** will be kinetically increased and could explain the progressive reduction of **1**.^{5,15} 2) Deprotonation of the DMF by **Cb-1** leading to the formation of a formamide-derived electron donor could also be a competitive pathway for the electron transfer.¹⁶ The unfavorable formation of **OED-1** and the poor conversion (12%) obtained with **IMe-CO₂** in *N,N*-dimethylacetamide (DMA)¹⁷ (Table 5, entry 5) would point mainly toward the formation of a formamide-derived OED.

Table 5. Mechanistic study.^[a]

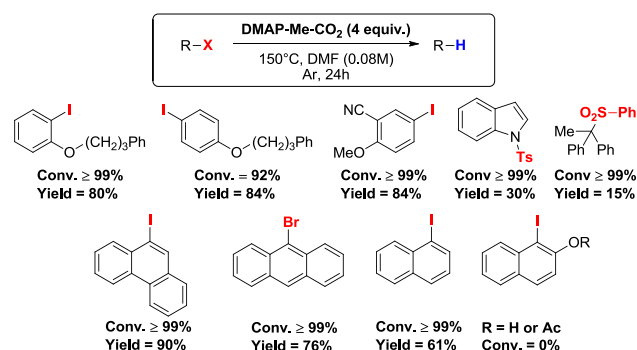
| Entry | Reducer | Equiv. | Temperature (°C) | Conv. (%) ^[b] |
|------------------|--|---------|------------------|--------------------------|
| 1 | OED-2 | 1.5 | 25 | 96 |
| 2 | Cb-1 | 3 | 25 | <4 |
| 3 | Cb-1 | 3 | 150 | 66 |
| 4 ^[c] | DMAP-Me-CO₂ | 3 | 150 | 99 |
| 5 ^[c] | IMe-CO₂ | 3 | 150 | 12 |
| 6 | DMAP-Me-CO₂ + TEMPO | 3 + 1.5 | 150 | 59 |
| 7 | DMAP-Me-CO₂ + <i>p</i>-DNB | 3 + 1.5 | 150 | 18 |
| 8 | DMAP-Me-CO₂ + air | 3 | 150 | 38 |

[a] **1** (1 equiv.), reducer (1.5 or 3 equiv.), DMF (0.08 M), Ar, 24h. [b] ¹H NMR conversion. [c] DMA (0.08M).

A different mechanism appears to operate with **DMAP-Me-CO₂**. The highly stable dimeric **OED-2** is probably the major generated form. Conservation of the reactivity in DMA (Table 5, entry 4) excludes the formation of a formamide-derived OED. Evidences supporting the electron transfer mechanism were obtained with the addition of commonly used inhibitors. The reduction of **1** decreased to 59% in the presence of the radical trap TEMPO (2,2,6,6-tetramethyl-1-piperidinyloxy), 18% with the competitive electron acceptor *p*-DNB (*para*-dinitrobenzene) and 38% when the reaction was carried out in air (Entries 6-8). Finally, analysis of the residual compounds at the end of the reaction confirmed the *in-situ* formation of the bispyridinylidene **OED-2** (Scheme 2). The same dimethylamino-pyridinium salt **DMAP-Me-X** was recovered from the aqueous phase starting either from the active form **OED-2**¹¹ or the carboxylate precursor. This pyridinium salt **DMAP-Me-X** probably arise from the thermal decomposition of the oxidized form **OED-2**²⁺. From a kinetic point of view, it seems that the first step of decarboxylation is the limiting step with a thermodynamic equilibrium between the **OED-2** and the carboxylate form **DMAP-Me-CO₂**. CO₂ remains in the DMF solution and competes with substrate **1** toward **OED-2**.¹¹

Scope of the reaction

To further investigate the versatility of our masked OED-system, the reduction of various substrates commonly used in OED-promoted reactions was examined.^{1,18} To our delight, we totally and cleanly reduced aryl halide, sulfone, or sulfonamide derivatives (Scheme 4). Beside the required precursor's activation temperature, the potency of **OED-2** was maintained using the same reaction conditions that previously reported (reducer loading, time, conversion). **DMAP-Me-CO₂** allowed the generation of **OED-2** in the presence of the substrate, contrary to pre-formulated strong base/azolium salt solutions.⁵ In addition, the reaction could be conveniently set-up in air and degassed under N₂ before heating. The few low isolated yields were attributed to the volatility of the reduced products. Iodonaphtol and its acetate counterpart were not reduced, but both led to the recovery of iodonaphtol. The competitive nucleophilic nature of **OED-2**^{1,19} certainly prevented the reduction in favor of the deprotonation of the alcohol or the deprotection of the acetate.



Scheme 4. Scope of the reaction.

In conclusion, we presented here an original concept of base-free generation of organic electron donors from air- and moisture-stable precursors. Newly synthesized aminopyridinium carboxylate and carbonate adducts were fully characterized. They presented interesting structural and electronic properties compared to imidazolium series. These pyridinium carboxylate and carbonate adducts could also provide access to original pyridinylidene ligands in organometallic chemistry. In our case, the aminopyridinium carboxylates proved to be excellent OED-precursors allowing the same order of reduction than the powerful organic reducers. These OED-masked systems will doubtless facilitate the handling of oxygen sensitive and elusive organic reducers and encourage their broader use. Work is now in progress to develop new OED-precursors with further enhanced functionality and practicality.

Acknowledgements

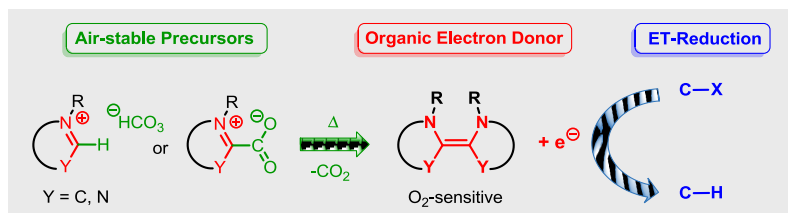
Aix-Marseille Université (AMU) and the Centre National de la Recherche Scientifique (CNRS) are gratefully acknowledged for financial support. G. T. thanks the Ministère de l'enseignement supérieur et de la recherche for his Ph.D. grant and P. N. thanks the Institut de Chimie Radicalaire for his master internship grant. We warmly thank Dr. Vincent Remusat for NMR analyses and the Spectropole (Fédération des Sciences Chimiques de Marseille) for MS, elemental analyses and X-ray determination. Our thanks to Michel Giorgi for valuable discussions on X-ray analysis.

Keywords: Electron transfer • organic electron donor • reduction reaction • carboxylate adduct • decarboxylation

- [1] For reviews, see: a) J. Broggi, T. Terme, P. Vanelle, *Angew. Chem.* **2014**, *126*, 392-423, *Angew. Chem. Int. Ed.* **2014**, *53*, 384-413; b) J.A. Murphy in *Encyclopedia of Radicals in Chemistry, Biology and Materials* (Eds.: C. Chatgililoglu, A. Studer), Wiley-VCH, Weinheim, **2012**; c) S. Zhou, H. Farwaha, J.A. Murphy, *Chimia* **2012**, *66*, 418-424; d) J.A. Murphy, *J. Org. Chem.* **2014**, *79*, 3731-3746; e) E. Doni, J.A. Murphy, *Chem. Commun.* **2014**, *50*, 6073-6087.
- [2] a) S.S. Hanson, N.A. Richard, C.A. Dyker, *Chem. Eur. J.* **2015**, *21*, 8052-8055; b) S.S. Hanson, E. Doni, K.T. Traboulsee, G. Coulthard, J.A. Murphy, C.A. Dyker, *Angew. Chem.* **2015**, *127*, 11388-11391, *Angew. Chem. Int. Ed.* **2015**, *54*, 11236-11239; c) H.S. Farwaha, G. Bucher, J.A. Murphy, *Org. Biomol. Chem.* **2013**, *11*, 8073-8081; d) E. Doni, S. O'Sullivan, J.A. Murphy, *Angew. Chem.* **2013**, *125*, 2295-2298, *Angew. Chem. Int. Ed.* **2013**, *52*, 2239-2242; e) E. Doni, B. Mondal, S. O'Sullivan, T. Tuttle, J.A. Murphy, *J. Am. Chem. Soc.* **2013**, *135*, 10934-10937; f) E. Cahard, F. Schoenebeck, J. Garnier, S.P.Y. Cutulic, S. Zhou, J.A. Murphy, *Angew. Chem.* **2012**, *124*, 3733-3736, *Angew. Chem., Int. Ed.* **2012**, *51*, 3673-3676.
- [3] a) M. Rueping, P. Nikolaienko, Y. Lebedev, A. Adams, *Green Chem.* **2017**, *19*, 2571-2575; b) Y. Su, Y. Li, R. Ganguly, R. Kinjo *Chem. Sci.* **2017**, *8*, 7419-7423; c) F. Cumine, S. Zhou, T. Tuttle, J.A. Murphy, *Org. Biomol. Chem.* **2017**, *15*, 3324-3336; d) Y. Liu, J. Xu, J. Zhang, X. Xu, Z. Jin, *Org. Lett.* **2017**, *19*, 5709-5712; e) M. Li, S. Berritt, L. Matuszewski, G. Deng, A. Pascual-Escudero, G.B. Panetti, M. Poznik, X. Yang, J.J. Chruma, P.J. Walsh, *J. Am. Chem. Soc.* **2017**, *139*, 16327-16333; f) D. Munz, J. Chu, M. Melaimi, G. Bertrand, *Angew. Chem.* **2016**, *128*, 13078-13082, *Angew. Chem. Int. Ed.* **2016**, *55*, 12886-12890; g) J. Broggi, M. Rollet, J.L. Clément, G. Canard, T. Terme, D. Gimes, P. Vanelle, *Angew. Chem.* **2016**, *128*, 6098-6103, *Angew. Chem. Int. Ed.* **2016**, *55*, 5994-5999; h) J.P. Barham, G. Coulthard, K. J. Emery, E. Doni, F. Cumine, G. Nocera, M.P. John, L.E.A. Berlouis, T. McGuire, T. Tuttle, J.A. Murphy, *J. Am. Chem. Soc.* **2016**, *138*, 7402-7410; i) J.P. Barham, G. Coulthard, R.G. Kane, N. Delgado, M.P. John, J.A. Murphy, *Angew. Chem.* **2016**, *128*, 4568-4572, *Angew. Chem. Int. Ed.* **2016**, *55*, 4492-4496; j) R. Rayala, A. Giuglio-Tonolo, J. Broggi, T. Terme, P. Vanelle, P. Theard, M. Médebielle, S.F. Wnuk, *Tetrahedron* **2016**, *72*, 1969-1977.
- [4] a) J.A. Murphy, J. Garnier, S.R. Park, F. Schoenebeck, S.-Z. Zhou, A.T. Turner, *Org. Lett.* **2008**, *10*, 1227-1230; b) J. Garnier, J.A. Murphy, S.-Z. Zhou, A.T. Turner, *Synlett* **2008**, 2127-2131.
- [5] a) P.I. Jolly, S. Zhou, D.W. Thomson, J. Garnier, J.A. Parkinson, T. Tuttle, J.A. Murphy, *Chem. Sci.* **2012**, *3*, 1675-1679; b) T.A. Taton, P. Chen, *Angew. Chem.* **1996**, *108*, 1098-1100, *Angew. Chem., Int. Ed. Engl.* **1996**, *35*, 1011-1013.
- [6] a) L. Delaude, *Eur. J. Inorg. Chem.* **2009**, 1681-1699; b) L. Yang, H. Wang, *ChemSusChem* **2014**, *7*, 962-998.
- [7] a) J.D. Holbrey, W.M. Reichert, I. Tkatchenko, E. Bouajila, O. Walter, I. Tommasi, R.D. Rogers, *Chem. Commun.* **2003**, 28-29; b) A.M. Voutchkova, M. Feliz, E. Clot, O. Eisenstein, R.H. Crabtree, *J. Am. Chem. Soc.* **2007**, *129*, 12834-12846.
- [8] B.R. Van Ausdall, J.L. Glass, K.M. Wiggins, A.M. Aarif, J. Louie, *J. Org. Chem.* **2009**, *74*, 7935-7942.
- [9] a) M. Fevre, J. Pinaud, A. Leteneur, Y. Gnanou, J. Vignolle, D. Taton, K. Miqueu, J.-M. Sotiropoulos, *J. Am. Chem. Soc.* **2012**, *134*, 6776-6784; b) M. Fevre, P. Coupillaud, K. Miqueu, J.-M. Sotiropoulos, J. Vignolle, D. Taton, *J. Org. Chem.* **2012**, *77*, 10135-10144.
- [10] E. Theuergarten, T. Bannenberg, M.D. Walter, D. Holschumacher, M. Freytag, C.G. Daniliuc, P.G. Jones, M. Tamm, *Dalton Trans.* **2014**, *43*, 1651-1662.
- [11] See supporting information for more details.
- [12] In solution, the decarboxylation temperature of carboxylate adducts is strongly influenced by the solvent polarity: D.M. Denning, D.E. Falvey *J. Org. Chem.* **2014**, *79*, 4293-4299.
- [13] Note that our Biotage® Initiator microwave system operates with sealed vials, not allowing the CO₂ evacuation.
- [14] C-F Bond activation by NHC, leading to the nucleophilic aromatic substitution of highly activated perfluorinated arenes, is reported: J. Emerson-King, S.A. Hauser, A.B. Chaplin, *Org. Biomol. Chem.* **2017**, *15*, 787-789 and references cited therein.
- [15] Although formation of **OED-1** is kinetically and thermodynamically unfavorable, evidences of the Wanzlick equilibrium in solution between enetetramine and carbene have been reported. a) R.W. Alder, M.E. Blake, L. Chaker, J.N. Harvey, F. Paolini, J. Schütz, *Angew. Chem.* **2004**, *116*, 6020-6036, *Angew. Chem. Int. Ed.* **2004**, *43*, 5896-5911; b) F.E. Hahn, L. Wittenbecher, D. Le Van, R. Fröhlich, *Angew. Chem.* **2000**, *112*, 551-554, *Angew. Chem. Int. Ed.* **2000**, *39*, 541-544. The activation energy for the dimerization of **Cb-1** was estimated at 23.4 kcal.mol⁻¹, reduced to 15.9 kcal.mol⁻¹ under electrophilic catalysis; c) M.-J. Cheng, C.-H. Hu, *Chem. Phys. Lett.* **2001**, *349*, 477-482; d) D.C. Graham, K.J. Cavell, B.F. Yates, *J. Phys. Org. Chem.* **2005**, *18*, 298-309.
- [16] For the formation of a DMF-derived organic donor upon deprotonation at 130°C with KO^tBu (pK_a (KO^tBu in DMSO) = 29.4 versus predicted pK_a (**Cb-1** in DMSO) = 21), see reference 3h.
- [17] *N,N*-Dimethylacetamide (DMA) does not allow the *in-situ* formation of OED upon its deprotonation.
- [18] F. Schoenebeck, J.A. Murphy, S.-Z. Zhou, Y. Uenoyama, Y. Miclo, T. Tuttle, *J. Am. Chem. Soc.* **2007**, *129*, 13368-13369.
- [19] N. Wiberg, *Angew. Chem.* **1968**, *80*, 809-822, *Angew. Chem. Int. Ed. Engl.* **1968**, *7*, 766-779.

Layout 2:

COMMUNICATION



Guillaume Tintori, Pierre Nabokoff,
Ruqaya Buhaibeh, David Bergé-Lefranc,
Sébastien Redon, Julie Broggi* and
Patrice Vanelle*

Page No. – Page No.

**Base-free generation of organic
electron donors from air-stable
precursors**

To enhance the practicality of organic electron donors (OED), new air- and moisture-stable carboxylate and carbonate precursors were synthesized and thermally activated to *in-situ* generate the potent electron donor. Carboxylate adducts proved to be excellent OED-latent systems, allowing the easy and efficient reduction of challenging substrates.